Accurate calibration of RL shunts for piezoelectric vibration damping of flexible structures

Høgsberg, Jan Becker; Krenk, Steen

Published in:
Proceedings of the 27th International Conference on Adaptive Structures and Technologies (ICAST 2016)

Publication date:
2016

Document Version
Peer reviewed version

ICAST2016: 27th International Conference on Adaptive Structures and Technologies
October 3-5, 2016, Lake George, New York, USA

Accurate calibration of RL shunts for piezoelectric vibration damping of flexible structures

Jan Høgsberg and Steen Krenk

Department of Mechanical Engineering, Technical University of Denmark, Kongens Lyngby, Denmark.

Abstract

Piezoelectric RL (resistive-inductive) shunts are passive resonant devices used for damping of dominant vibration modes of a flexible structure and their efficiency relies on precise calibration of the shunt components. In the present paper improved calibration accuracy is attained by an extension of the local piezoelectric transducer displacement by two additional terms, representing the flexibility and inertia contributions from the residual vibration modes, not explicitly targeted by the shunt damping. This results in an augmented dynamic model for the targeted resonant vibration mode, in which the residual contributions, represented by two correction factors, modify both the apparent transducer capacitance and the shunt impedance. Explicit expressions for the correction of the shunt circuit inductance and resistance are presented in a form that is generally applicable to calibration formulae derived on the basis of an assumed single-mode structure, in which the modal interaction has been deliberately neglected. A design procedure is devised and subsequently verified by numerical examples, demonstrating that effective mitigation can be obtained for an arbitrary vibration mode when the residual mode correction is included in the calibration of the *RL* shunt.

1. INTRODUCTION

Piezoelectric resistive-inductive (RL) shunt damping is a robust concept for response mitigation of flexible structures, as it passively targets the dominant vibration modes of the structure by a supplemental resonance introduced by the shunt inductance that is calibrated accurately such that the shunt resistance can optimally dissipate the vibration energy. The efficiency of resonant RL shunt damping depends on a precise calibration of the supplemental system frequency and energy outtake. Numerous design approaches and calibration formulae have been derived in for example [1] - [8], based on the assumption that the vibrating structure is sufficiently described by its dominant resonant mode. However, piezoelectric transducers are commonly placed locally on a flexible structure, thereby activating residual modes not specifically addressed by the shunt damping approach. In Fig. 1 a piezoelectric laminate transducer acts on the bending deformation of a cantilever, thus in principle activating all vibration modes of the flexible beam structure. The energy spill-over from residual modes changes the closed-loop dynamics of the structure and thus deteriorates the performance when using calibration principles based on an assumed structural response with only a single mode shape, hereby neglecting any modal interaction

* Corresponding author, jhg@mek.dtu.dk

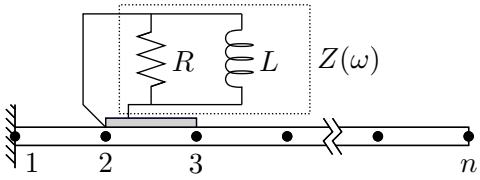

Figure 1: Discretized beam with piezoelectric shunt system.

inherently present in the original flexible structure with multiple modes. A calibration approach has been presented in [9] for RL shunts, based on a quasi-static representation of the residual mode effects.

In vibration problems commonly addressed by piezoelectric RL shunts the largest energy content can furthermore occur in intermediate vibration modes, as for example in the case of acoustic vibrations of membranes and plates. In the underlying calibration procedures a correction with respect to non-resonant modes both below and above the targeted resonance may therefore be needed. Recently, a consistent correction format has been proposed by Krenk and Høgsberg [10], where both flexibility and inertia contributions from the non-resonant modes have been represented. In the present paper this consistent residual mode correction is formulated in the context of piezoelectric RL shunt damping, based on the theoretical results in [11]. It is demonstrated that general expressions for the correction of the shunt inductor (L) and resistor (R) can be obtained in explicit form, making the present approach generic and thus applicable to a large variety of calibration formulae and principles derived on the basis of a simplified single-mode structure, where the modal interaction is present because the piezoelectric transducer acts locally on the flexible structures.

2. ELECTROMECHANICAL STRUCTURE

Piezoelectric RL shunts are effectively applied for passive damping of flexible structures exposed to resonant loading. In the present section the governing equations of the flexible structure and the corresponding modal properties are initially derived, followed by a brief introduction to the piezoelectric forcing. Finally, the performance of single-mode calibration is illustrated for the parallel RL shunt.

2.1 Flexible structure

The equation of motion of the vibrating structure to be damped by the piezoelectric transducer force f can be written in the frequency domain as

$$\big(-\omega^2\mathbf{M} + \mathbf{K}\big)\mathbf{u} + \mathbf{w}f = \mathbf{f}_e \tag{1}$$

where ω is the driving frequency of the harmonic loading with amplitude vector $\mathbf{f}_e$. In this equation of motion the complex vibration amplitudes are contained in vector $\mathbf{u}$, while $\mathbf{M}$ and $\mathbf{K}$ are the corresponding mass and stiffness matrix of the structure with short-circuit transducer electrodes. The placement of the transducer on the structure is represented by the connectivity vector $\mathbf{w}$, which therefore simultaneously determines the transducer displacement as

$$u = \mathbf{w}^{\mathrm{T}}\mathbf{u} \tag{2}$$

Thus, the displacement u is by construction complementary with respect to work to the applied transducer force f.

Resonant vibration absorbers are calibrated with respect to the properties of the resonant vibration mode of the structure. The mode shape $\mathbf{u}_j$ and natural angular frequency ω_j of the vibrating host structure are governed by the generalized eigenvalue problem associated with the homogeneous form of (1),

$$\big(\mathbf{K} - \omega_j^2\mathbf{M}\big)\mathbf{u}_j = \mathbf{0} \tag{3}$$

The calibration of the vibration absorber is conveniently based on a vibration form that is normalized to unity at the location of the transducer. The modal representation can therefore be written as

$$\mathbf{u} = \sum_j \frac{\mathbf{u}_j}{\mathbf{w}^{\mathrm{T}}\mathbf{u}_j} u_j \tag{4}$$

and the modal equation of motion is then subsequently obtained from (1) as

$$(-\omega^2 m_j + k_j)u_j + f = f_j \tag{5}$$

in which modal mass, modal stiffness and modal load are defined as

$$m_j = \frac{\mathbf{u}_j^{\mathrm{T}}\mathbf{M}\mathbf{u}_j}{(\mathbf{w}^{\mathrm{T}}\mathbf{u}_j)^2} \quad , \quad k_j = \frac{\mathbf{u}_j^{\mathrm{T}}\mathbf{K}\mathbf{u}_j}{(\mathbf{w}^{\mathrm{T}}\mathbf{u}_j)^2} \quad , \quad f_j = \frac{\mathbf{u}_j^{\mathrm{T}}\mathbf{f}_e}{\mathbf{w}^{\mathrm{T}}\mathbf{u}_j} \tag{6}$$

The particular normalization in the summation in (4) secures that the transducer force f appears explicitly in the modal equation of motion (5), which is convenient in connection with the shunt calibration in Section 3.

2.2 The piezoelectric force

The piezoelectric transducer force f is proportional to the voltage V across the electrodes,

$$f = \theta V \tag{7}$$

introducing the electromechanical coupling coefficient θ. The coupling effect is represented by the sensor equation

$$Q = -\theta u + CV \tag{8}$$

where Q is the charge in the transducer, while C is the capacitance associated with $u = 0$. Finally, the charge is related to the voltage via the impedance $Z(\omega)$ of the supplemental shunt,

$$V = -i\omega Z(\omega) Q \tag{9}$$

Elimination of Q between (8) and (9), followed by substitution of the resulting equation (9) into (7) gives the apparent mechanical flexibility relation

$$u = \left(\frac{C}{\theta^2} + \frac{1}{i\omega\theta^2 Z(\omega)}\right) f \tag{10}$$

in which the capacitance-term represents an apparent spring with stiffness θ^2/C, while the impedance function defines a viscous dashpot with frequency dependent viscous coefficient $\theta^2 Z(\omega)$. The present

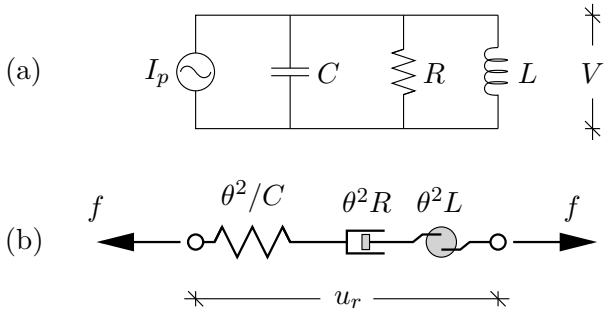

Figure 2: Equivalent models of piezoelectric transducer with parallel shun.

study concerns the calibration of resonant RL shunts, where the series and parallel configurations have been introduced in [1] and [2], respectively. The impedance function for the parallel RL shunt is conveniently formulated in terms of the individual reciprocal parameters,

$$\frac{1}{Z(\omega)} = \frac{1}{R} + \frac{1}{i\omega L} \tag{11}$$

The electrical model of the piezoelectric shunt system is shown in Fig. 2(a), with all three components placed in parallel. By substitution of (11) into (10) the flexibility relation (10) can be written as

$$u = \left(\frac{C}{\theta^2} + \frac{1}{i\omega\theta^2 R} - \frac{1}{\omega^2\theta^2 L} \right) f \tag{12}$$

This relation between force f and displacement u corresponds to the mechanical transducer model in Fig. 2(b), with a spring, damper and inerter placed in series. As demonstrated next the residual mode contributions are also additive in terms of flexibilities, and they are therefore directly absorbed by the electrical components in Fig. 2(a). For the series RL shunt the residual mode contributions can not be combined exactly with the shunt components, but as demonstrated in [11] consistent approximations lead to explicit and accurate solutions.

2.3 Single-mode calibration

Numerous design principles and procedures are available for the components of both series and parallel RL shunts. Table 1 summarizes some basic calibration formulae for the normalized inductance and resistance,

$$\lambda_r = LC\omega_r^2 \qquad , \qquad \rho_r = RC\omega_r \tag{13}$$

In the maximum damping calibration [4] the inductance λ_r is determined to create equal modal damping in the two modes of the assumed single-mode structure, while the resistance is chosen according to the bifurcation point of the two complex roots. However, maximum damping is not equivalent to optimal response mitigation, since the two vibration modes at the bifurcation point experience constructive interference [1]. Thus, the minimum amplitude calibration derived in [2] leads to alternative expressions for λ_r and ρ_r, as seen in row two of Table 1. Conversely, equal modal damping is not obtained by the minimum amplitude calibration, although it is a robust design property that it is independent of the

Table 1: Single-mode calibration of parallel RL shunt.

	λ_r	ρ_r
Maximum damping	1	$\sqrt{\frac{1}{4\kappa_r}}$
Minimum amplitude	$\frac{1}{1-\frac{1}{2}\kappa_r}$	$\sqrt{\frac{1}{2\kappa_r}}$
Balanced calibration	1	$\sqrt{\frac{1}{2\kappa_r}}$

particular loading condition. The balanced calibration principle introduced in [7] for piezoelectric RL shunt damping determines the inductance λ_r based on equal damping, while the resistance ρ_r is chosen $\sqrt{2}$ smaller than the value associated with the bifurcation point to avoid the interference. This principle has been derived for the mechanical tuned mass damper [12], for which the classic frequency calibration actually corresponds to equal damping of the two modes. The balanced calibration finally gives an explicit relation between the gain or coupling parameter κ_r of the resonant system and the attainable level of modal damping ζ_{des},

$$\kappa_r = 8\zeta_{\text{des}}^2 \tag{14}$$

This simple relation constitutes a suitable starting point for a consistent design procedure based on ζ_{des}, while the optimal inductance and resistance are then determined from the expressions summarized in Table 1. Thus, in the following results are determined by the balanced calibration. The corresponding calibration formulae for the series RL shunt may be obtained from [4] or [11].

In most shunt calibration procedures the RL shunt is calibrated based on the system properties of the structure, where the displacement u is approximated by the modal displacement of the targeted vibration form: $u_r = \mathbf{w}^T \mathbf{u}_r$. However, this ignores the modal interaction with the vibration modes of the flexible structure, not targeted by the shunt damping. Figure 3 shows the frequency response curves for the tip deflection of the structure in Fig. 1. The blue dashed curves are the actual response amplitudes of the flexible structure when loaded by the modal load distribution, while the red solid curves represent the

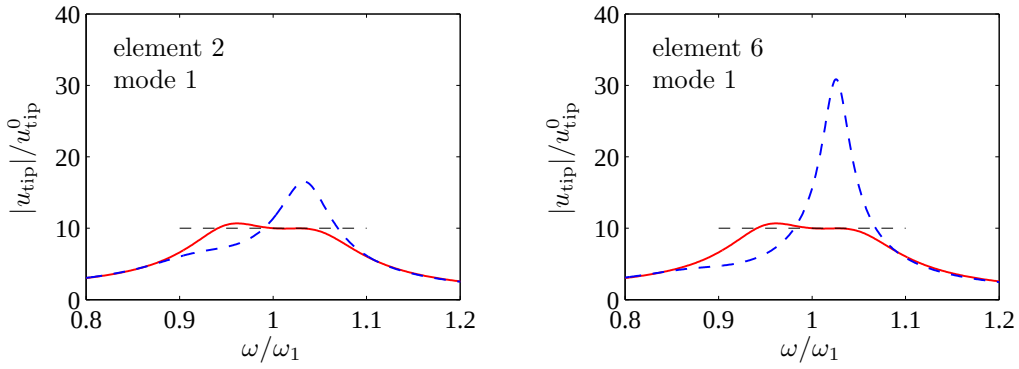

Figure 3: Dynamic amplification curve for transducer placed at element 2 and 6.

desired solution obtained by the balanced calibration procedure for an idealized single mode structure. It is seen that a severe detuning of the calibration occurs because of the local transducer placement on a flexible structure. In the following the interaction with the residual vibration modes is taken into account by a consistent augmentation of the transducer displacement, whereby the frequency response curves retain the properties of the desired (red) curves in Fig. 3. The desired damping level for the calibration in the figure is $\zeta_{\rm des} = 0.05$, and the dynamic amplification factor of the optimal (red) curve corresponds almost exactly to $DAF = 1/(2\zeta_{\rm des}) = 10$.

3. SHUNT CALIBRATION

The substantial detuning experienced for the calibration of piezoelectric RL shunt damping acting on a flexible structure is due to the modal interaction introduced by the local attachment of the transducer. If the spatial distribution of the transducer can not be sufficiently aligned with the shape of the resonant vibration form, the interaction with the residual vibration modes must instead be taken into account via the calibration procedure. An augmented modal analysis is now presented, leading to explicit corrections of the calibration formulae for the parallel RL shunt components.

3.1 Augmented modal representation

The single-mode approximation $u = u_r$ is often inadequate because the displacement u in (2) contains contributions from both the targeted resonant mode ($j = r$) and the other residual modes ($j \neq r$). As recently demonstrated in [10] the influence of the interaction with the non-resonant modes may instead be represented by the augmented modal representation

$$u_r = u + \left(\frac{1}{k_r'} - \frac{\omega_r^2}{\omega^2} \frac{1}{k_r''} \right) f \tag{15}$$

The residual mode flexibility coefficients inside the parenthesis are effectively computed as

$$\frac{1}{k_r'} = \mathbf{w}^{\rm T} \mathbf{K}_r^{-1} \mathbf{w} - \frac{1}{k_r} + \frac{1}{k_r''} \qquad , \qquad \frac{1}{k_r''} = \mathbf{w}^{\rm T} \mathbf{K}_r^{-1} \mathbf{K} \mathbf{K}_r^{-1} \mathbf{w} - \mathbf{w}^{\rm T} \mathbf{K}_r^{-1} \mathbf{w} \tag{16}$$

where the modified stiffness matrix $\mathbf{K}_r$ is shifted by the inertia contained in the resonant vibration mode,

$$\mathbf{K}_r = \mathbf{K} - \omega_r^2 \left(\mathbf{M} - \frac{(\mathbf{M}\mathbf{u}_r)(\mathbf{M}\mathbf{u}_r)^{\rm T}}{\mathbf{u}_r^{\rm T} \mathbf{M} \mathbf{u}_r} \right) \tag{17}$$

It is observed that the resonant mode dynamics are not altered by this modification of the stiffness matrix, as verified by the modal stiffness $\mathbf{u}_r^T \mathbf{K}_r \mathbf{u}_r = \mathbf{u}_r^T \mathbf{K} \mathbf{u}_r = k_r$. As demonstrated in detail in [10] both the flexibility coefficient $1/k_r'$ and the corresponding inertia coefficient $1/k_r''$ are non-negative whereby the total residual mode contribution is consistently divided into the two supplemental contributions inside the parenthesis in (15).

3.2 Equivalent mechanical model

The modal force-displacement relation, representing the mechanical characteristics of the piezoelectric shunt damper, are now obtained by substitution of (15) into (12). The augmented modal force

equation can then be written as

$$\Big(\frac{C}{\theta^2}+\frac{1}{i\omega\theta^2 R}-\frac{1}{\omega^2\theta^2 L}+\frac{C'}{\theta^2}-\frac{1}{\omega^2\theta^2 L''_r}\Big)f = u_r \tag{18}$$

where the residual mode flexibility and inertia terms can be represented by a supplemental capacitance and inductance,

$$C'_r = \frac{\theta^2}{k'_r} \quad , \quad L''_r = \frac{k''_r}{\omega_r^2\theta^2} \tag{19}$$

The two capacitance and inductance terms in the model can be combined to introduce equivalent single modal parameters

$$C_r = C + C'_r \qquad , \qquad \frac{1}{L_r} = \frac{1}{L} + \frac{1}{L''_r} \tag{20}$$

Thus, for the parallel RL shunt the residual mode corrections are directly absorbed by the electrical components.

3.3 Correction formulae

By the introduction of the modal capacitance C_r and inductance L_r in (20) the modal flexibility relation (18) reduces to a form similar to (12), but now with respect to the modal displacement u_r. In normalized form this relation can be written as

$$u_r = \Big(\frac{C_r}{\theta^2}+\frac{1}{i\omega\theta^2 R}-\frac{1}{\omega^2\theta^2 L_r}\Big)f = \Big(1+\frac{\omega_r}{i\omega}\frac{1}{\rho_r}-\frac{\omega_r^2}{\omega^2}\frac{1}{\lambda_r}\Big)\frac{f}{\kappa_r k_r} \tag{21}$$

introducing the modal electromechanical coupling coefficient

$$\kappa_r = \frac{\theta^2}{C_r k_r} \tag{22}$$

and the non-dimensional modal resistance and inductance

$$\lambda_r = L_r C_r \omega_r^2 \qquad , \qquad \rho_r = R C_r \omega_r \tag{23}$$

The calibration formulae for λ_r and ρ_r are determined on the basis of an equivalent single-mode structure and explicit expressions are summarized in Table 1 for some of the most common procedures.

Elimination of C_r and L_r in (23) by the definitions in (20) gives the following normalized expressions for the actual inductance L and resistance R for the parallel RL shunt,

$$LC\omega_r^2 = \frac{\lambda_r}{(1+\kappa'_r)(1-\kappa''_r\lambda_r)} \qquad , \qquad RC\omega_r = \frac{\rho_r}{(1+\kappa'_r)} \tag{24}$$

where the non-dimensional correction factors are introduced as

$$\kappa'_r = \frac{C'_r}{C} = \frac{\theta^2}{C k'_r} \qquad , \qquad \kappa''_r = \frac{1}{L''_r C_r \omega_r^2} = \frac{\theta^2}{C_r \kappa''_r} = \kappa_r \frac{k_r}{k''_r} \tag{25}$$

Thus, the calibration formulae introduced in Table 1 derived for an idealized single-mode structure can be explicitly corrected by (24) and thereby used for damping of flexible structures with substantial modal interaction.

A design procedure could be conducted as follows. Initially, a desired damping ratios $\zeta_{\rm des}$ is determined based on a preliminary dynamic analysis of the flexible structure. The corresponding modal coupling coefficient is estimated as $\kappa_r^2 = 8\zeta_{\rm des}$ and the piezoelectric transducer is deigned and located according to the non-dimensional parameter $\theta^2/C = k_r\kappa_r(1+\kappa_r')$. The equivalent single-mode shunt components λ_r and ρ_r are then determined from the preferred calibration principle (see Table 1) and the actual inductance and resistance are finally obtained by the corrections in (24). This procedure is illustrated by the numerical examples in the next section.

4. DAMPING OF CANTILEVER

Two simple examples are used to illustrate the accuracy of the shunt calibration when including the residual mode correction in (24). Initially the cantilever beam in Fig. 1 is investigated, with a laminate transducer covering a single beam element of the numerical model. A severe increase in vibration amplitude has already been identified in Fig. 3 for the pure single-mode calibration without residual mode correction. In the second example a piezoelectric stack transducer act as support instead, thus restraining the motion of the beam structure.

4.1 Laminate transducer

The cantilever in Fig. 1 is discretized by 20 plane beam elements with transverse displacement and cross section rotation as the two nodal degrees-of-freedom (dofs). The laminate transducer acts on the rotational dofs of a single finite element via the connectivity vector $\mathbf{w} = [0,\dots,0,-1,0,1,\dots,0]^T$ with non-zero entries at the two rotational dofs. The desired damping ratio is chosen as $\zeta_{\rm des} = 0.05$, whereby the electromechanical coupling parameter $\kappa_r = 8\zeta_{\rm des}^2 = 0.02$. The supplemental bending stiffness by the transducer is chosen as $100EI/\ell$, where EI and ℓ are the bending stiffness and the length of the cantilever, respectively. The single laminate transducer is placed at element 2 or 6, and damping is assessed both for modes 1 and 3. For damping of mode 1 the damping ratios associated with the resonant mode are $\zeta_1 = \{0.0499, 0.0499\}$ for both transducer locations, while for the assumed single-mode calibration the damping ratios of the flexible beam structure are $\zeta_1^0 = \{0.0676, 0.0274\}$ and $\{0.0752, 0.0144\}$ for elements 2 and 6, respectively. This corresponds to a reduction in attainable damping by around 50% and 30% compared to the desired value. For mode 3 the damping ratios obtained by the corrected calibration are $\zeta_3 = \{0.0500, 0.0499\}$ for both locations, while in the uncorrected case they are $\zeta_1^0 = \{0.0757, 0.0074\}$ (element 2) and $\zeta_1^0 = \{0.0743, 0.0157\}$ (element 6). For mode 3 at element 2 the authority of the laminate transducer is significantly limited, with a flexibility factor $\kappa_3' = 0.7464$ close to unity and a corresponding inertia coefficient $\kappa_r'' = 0.0119$ comparable in magnitude to the coupling parameter $\kappa_r = 0.0200$. Thus, for this configuration the smallest damping ratio is only 15% of the targeted value of 0.05. This shows that the residual mode correction is of great importance when the transducer is placed at indirect locations on the structure.

Figure 4 shows the frequency amplitude curves for the tip deflection of the cantilever for all combinations of modes 1 and 3 and (transducer locations at) elements 2 and 6. The two top figures for mode 1 correspond to those in Fig. 4 and it is seen that the amplitude curve obtained by the corrected calibration (solid blue line) exactly recovers the desired single-mode solution (solid red line) at the predicted $DAF = 10$ represented by the horizontal dashed line. As seen from both the damping ratios and the dynamic amplification curves the critical mode is the one with the smaller natural frequency, which indi-

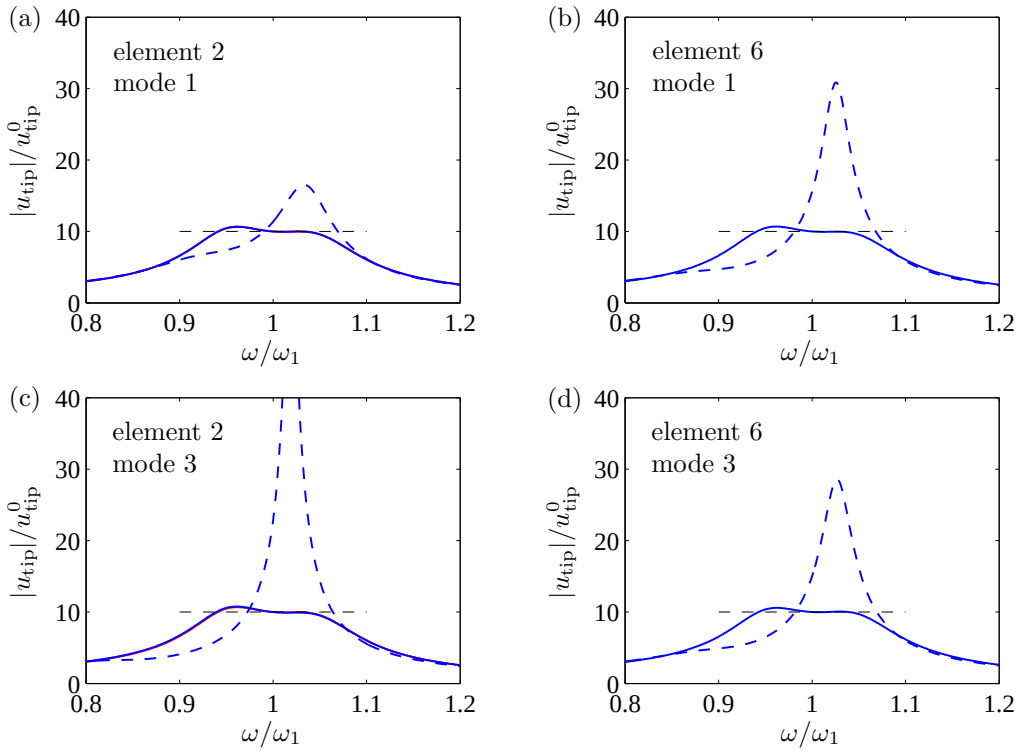

Figure 4: Dynamic amplification curve for transducer placed at element 2 (a) and 6 (b).

cates that the cantilever with a laminate transducer is mainly influenced by the quasi-static residual mode correction represented by κ_r', whereas the inertia correction factor κ_r'' has only limited influence in the present example.

4.2 Support transducer

In the second example a system is constructed where the inertia correction plays a more prominent role. This requires that the transducers acts directly on the transverse motion of the structure, as illustrated in Fig. 5 where a stack-type transducer transversely supports the free end of the cantilever. The axial stiffness of the stack transducer is $100EI/\ell^3$, which makes it sufficiently soft to allow enough transverse displacement at the right end to activate the inertia correction. For mode 1 the correction factors are $\kappa_r' = 0.0664$ and $\kappa_r'' = 0.0092$ and the calibration is therefore mostly influenced by the flexibility correction. However, for mode 4 the inertia coefficient $\kappa_r'' = 0.0803$ is almost two times larger than

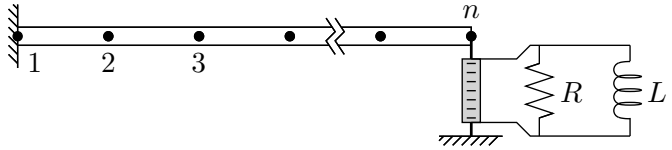

Figure 5: Cantilever with transverse transducer at free end.

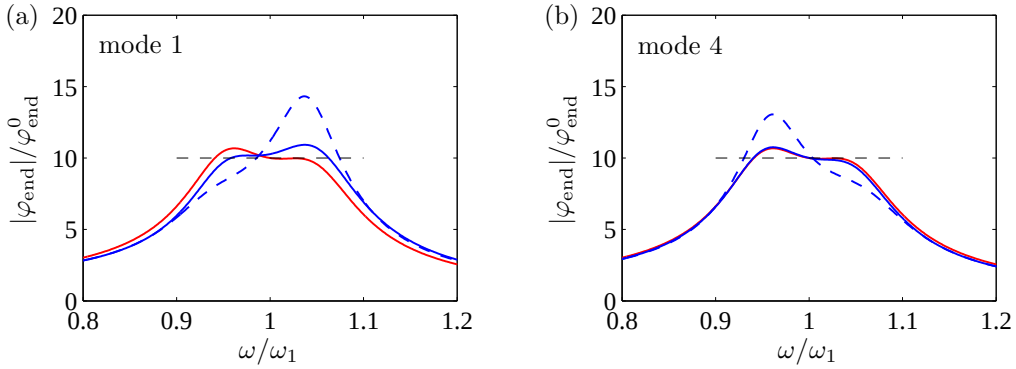

Figure 6: Dynamic amplification curve for transducer placed at right end.

$\kappa_r' = 0.0432$. Thus, for mode 4 the inertia correction constitutes the main contribution. For the two modes the desired damping ratios $\zeta_1 = \{0.0500, 0.0499\}$ and $\zeta_4 = \{0.0499, 0.0500\}$ are accurately obtained when the corrected calibration is applied, while in the case without correction ($\kappa_r' = 0$, $\kappa_r'' = 0$) the damping ratios are instead $\zeta_1^0 = \{0.0600, 0.0365\}$ and $\zeta_4^0 = \{0.0387, 0.0555\}$. For both modes the attainable damping is reduced by more than 25%. However, for mode 4 it is now the mode with smaller frequency that is reduced, indicating that inertia contributions from the lower residual modes (1 to 3) influence the dynamics of the resonant mode 4. This is also observed for the dynamic amplification curves for the end rotation $\varphi_{\rm end}$ in Fig. 6, where the undesirable amplification of the (dashed) curve without correction occurs for the right peak for mode 1, while for mode 4 the largest amplitude occurs for the left peak with smaller frequency.

5. CONCLUSIONS

The present paper improves the calibration accuracy for piezoelectric RL shunts by a consistent procedure taking into account the spill-over from the non-resonant modes of the flexible structure. The approach is based on the representation of the transducer displacement u in terms of the displacement of the resonant vibration mode u_r and two additional terms representing the flexibility and inertia contributions from the residual vibration modes of the structure. Hereby an equivalent single-mode structural model is established, in which the modal interaction with non-resonant modes is explicitly represented by two non-dimensional background flexibility and inertia coefficients κ_r' and κ_r'', that are directly available from the numerical model of the flexible structure. For piezoelectric shunt damping it is demonstrated that the residual mode flexibility is directly absorbed by the short-circuit transducer capacitance, while the inertia contribution is equivalent to a supplemental inductance and therefore directly combined with the actual inductance of the parallel RL shunt. By this reinterpretation of the piezoelectric shunt via the residual mode contributions a pair of explicit correction formulae for the shunt circuit inductance and resistance are obtained, and any set of calibration formulae for (parallel) RL shunts, derived on the basis of an assumed single-mode structure, can therefore be corrected to take into account the interaction with non-resonant modes. Finally, numerical examples verify the accurate shunt calibration, also for intermediate vibration forms, securing both equal damping of the targeted modes and effective response reduction by the pole placement based balanced calibration principle.

ACKNOWLEDGEMENTS

The financial support by *The Otto Mønsted Foundation* is gratefully acknowledged.

REFERENCES

1. Hagood, N.W. and von Flotow, A., "Damping of structural vibrations with piezoelectric materials and passive electrical networks", *Journal of Sound and Vibration*, Vol. 146, 1991, pp. 243-268.
2. Wu, S.Y., "Piezoelectric shunts with a parallel R-L circuit for structural damping and vibration control", *Proceedings of the SPIE*, Vol.2720, 1996, pp. 259-269.
3. Park, C.H. and Inman, D.J., "A uniform model for series R-L and parallel R-L shunt circuits and power consumption", *SPIE Proceedings*, Vol.3668, 1999, pp. 797-804.
4. Caruso, G., "A critical analysis of electric shunt circuits employed in piezoelectric passive vibration damping", *Smart Materials and Structures*, Vol.10, 2001, pp. 1059-1068.
5. Yamada, K., Matsuhisa, H. , Utsuno, H. and Sawada, K., "Optimum tuning of series and parallel LR circuits for passive vibration suppression using piezoelectric elements", *Journal of Sound and Vibration*, Vol.329, 2010, pp. 5036-5057.
6. Kozlowski, M.V., Cole, D.G. and Clark, R.L., "A comprehensive study of the RL series resonant shunted piezoelectric: A feedback controls perspective", *Journal of Vibration and Acoustics*, Vol.133, 2011, 011012 (10pp).
7. Høgsberg, J. and Krenk, S., "Balanced calibration of resonant shunt cicuits for piezoelectric vibration control", *Journal of Intelligent Material Systems and Structures*, Vol.23, 2012, pp. 1937-1948.
8. Soltani, P., Kerschen, G., Tondreau, G. and Deraemaeker, A., "Piezoelectric vibration damping using resonant shunt circuits: an exact solution", *Smart Materials and Structures*, Vol.23, 2014, 125014 (11pp).
9. Høgsberg, J. and Krenk, S., "Balanced calibration of resonant piezoelectric RL shunts with quasi-static background flexibility correction", *Journal of Sound and Vibration*, Vol.341, 2015, pp. 16-30.
10. Krenk, S.and Høgsberg, J., "Tuned resonant mass or inerter-based absorbers: unified calibration with quasi-dynamic flexibility and inertia correction", *Proceedings of the Royal Society A-Mathematical, Physical and Engineering Sciences*, Vol.472, 2015, 20150718 (23pp).
11. Høgsberg, J. and Krenk, S., "Calibration of piezoelectric *RL* shunts with explicit residual mode correction", *Submitted for publication*, 2016.
12. Krenk, S., "Frequency analysis of the tuned mass damper", *Journal of Applied Mechanics*, Vol.72, 2005, pp. 936-942.